DYNAMIC CHARACTERISTICS OF NANJING FLAKE-SHAPED SAND IN LONG-TERM REPEATED LOADING

LIU Xue-zhu[1,2] and CHEN Guo-xing[1]

[1] *Institute of Geotechnical Engineering, Nanjing University of Technology , Nanjing. China*
[2] *Geo-technical Engineering Company of Jiangsu Province, Nanjing, China*

ABSTRACT :

The flake-shaped sand soils, containing quartz, chlorite and muscovite minerals, are widely distributed throughout the middle and lower reaches of the Yangtze River. Comparing with the standard quartz sand soils composed of circular-shaped particles, the flake-shaped structural sand has some differences in physical mechanics properties. The flake-shaped particle components give rise to the anisotropic property in physical mechanics properties of flake-shaped structural sand, and its strength in horizontal direction is smaller than that of vertical direction. Moreover, some preliminary researches indicate that the flake-shaped structures have a large effect on liquidation properties of sand, and its dynamic shear modulus and damp properties also have marked differences from the standard quartz sand. So, a series of dynamic characteristics tests on flake-shaped sand was performed by using the WFI cyclic triaxial apparatus made in England. The dynamic characteristics of flake-shaped sand under different cell pressure, initial static deviator stress and axial cyclic stress ratio, were studied and its influence regularity was analyzed. In addition, through comparing the effective stress path under cyclic loading with static loading, the process of liquefaction of saturated Nanjing flake-shaped sand with development of dynamic pore-water pressure, including stable state, compression state, dilative state and dynamic stress-strain behavior, were investigated. And two kinds of failure patterns of saturated Nanjing flake-shaped sand were provided.

KEYWORDS: long-term repeated loading; Nangjing flake-shaped sand; dynamic characteristics; failure pattern; effective stress path

1. INTRODUCTION

Fine sand whose components was mainly flake-shaped particles was widely distributed along the middle and lower reaches of the Yangtze River, which contains quartz, chlorite and mica particles. And it is different from standard sand with round quartz particles usually used in the dynamic test. The nature of flake-shaped sand is anisotropic because of flake-shaped particles, and the strength of horizontal direction is lower than the strength of vertical direction. Academician Zhou Jing (1999) paid attention to the mechanical properties of flake-shaped sand firstly, and named it Nanjing sand. Chen Wen-hua etc. (2003) studied liquefaction characteristic of flake-shaped sand. Their research showed that the flake-shaped particle structure had an important effect on the liquefaction characteristic, and this flake-shaped particle structure must be considered when estimating liquefaction probability of this sand. Chen Guo-xing, etc. (2004) studied the dynamic characteristics of Nanjing sand by some indoor experiments, and the preliminary research results showed that the dynamic shear modulus and damping characteristics have significant difference between Nanjing flake-shaped fine sand and common quartz sand. However, the systematic and deep study on the dynamic characteristics of Nanjing fine sand is still lack.

Under repeated vibrating load induced by rapid rail transit, besides the influence of composition itself, the static deviator stress, cyclic stress ratio and cyclic numbers have great effect on the dynamic characteristic of sand soils such as dynamic strength, dynamic deformation and so on. When calculating the subgrade deformation, not only the characteristic and magnitudes of vehicle load but also the static deviator stress, the interaction between static deviator stress and dynamic stress need to be considered which have remarkable effect on long-term deformation. Therefore, the effect of the static deviator stress level and the dynamic level on the characteristic of saturated flake-shaped sand was studied in this paper. In addition, by combining static triaxial compression test, the development process of the effective stress path and failure pattern were investigated under repeated vibrating load induced by rapid rail transit. This investigation may have great significance for design and construction of rail transit roadbed projects.

2. SOIL SAMPLES AND TEST METHODS

2.1. Soil Samples

Static triaxial compression tests and cyclic triaxial tests were carried out using the WFI cyclic triaxial system. The soil samples, taken from the Xu fu xiang station site of Nanjing Metro, are flaked-shaped fine sand, which is gray with densities from medium compactness to compactness. Its morphogenesis belongs to the Yangtze River floodplain and ancient river accumulation. And liquation phenomenon may occur under dynamic loading. The sand soils contain some quartz particles, small number of chlorite, muscovite, clay sliver and weathered heavy minerals. The proportion of quartz particles in sand is from 50% to 60%. There are some differences between Nanjing flake-shaped sand and the circular particle standard quartz sand in particle composition and gradation. Compared with Fujian standard sand, Nanjing sand is much looser, its void ratio and density are bigger and the average particle size is smaller. The soil samples had following mechanical indexes: the average nature density $\rho = 18.5kN/m^3$, the maximum void ratio $e_{\max} = 1.14$, the minimum void ratio $e_{\min} = 0.62$, relative density $D_r = 0.5$, uniformity coefficient Cu=2.31 and curvature coefficient Cc=1.07. The height and diameter of the soil sample is 8.0cm and 3.91cm respectively. The particle size distribution curve of Nanjing flake-shaped fine sand is shown in Figure 1.

2.2. Cyclic Triaxial Test Methods

There are two test schemes to consider the effect of static deviator stress on the dynamic of saturation flake-shaped sand. One scheme is that static deviator stress is applied under entire drainage conditions, then static deviator stress completely transformed into effective stress before cyclic load applied, in other words, the dynamic stress is applied after the soil has completely consolidated under static deviator stress. The other scheme is that static deviator stress is applied under undrained condition and more specifically the dynamic stress is immediately applied to the subgrade soil after static deviator stress applied. However, It is worthy to

note that the practical situation is between the drainage condition and undrained condition. According to whether exist the initial static deviator stress conditions and the deviator stress reverse after imposed cyclic load, the cyclic triaxial test can be divided into three situations: (1) $q_s / p_c^{'} = 0$ and $q_{cyc} > q_s$,(2) $q_s / p_c^{'} > 0$ and $q_{cyc} > q_s$, (3) $q_s / p_c^{'} > 0$ and $q_{cyc} < q_s$, as shown in table 1.

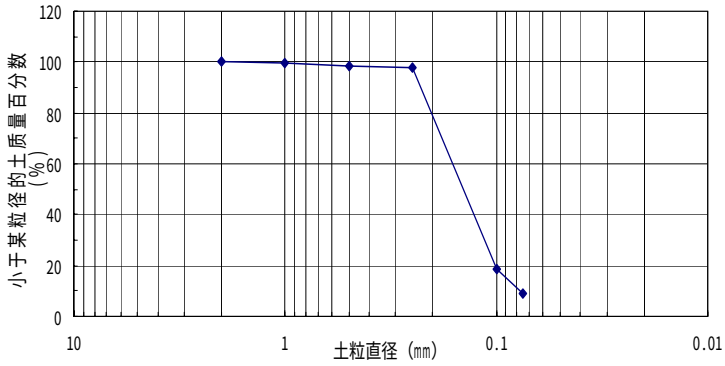

Figure1 Particle size distribution curve of Nanjing flake-shaped fine sand

Table 1. Details of undrained cyclic triaxial tests under different static deviator stress

Number	static deviator stress q_s (kPa)	static deviator stress ratio $q_s / p_c^{'}$	Dynamic deviator stress q_{cyc} (kPa)	Dynamic deviator stress ratio $q_{cyc} / p_c^{'}$	Stress reversal
0-1			18	0.18	
0-2	0	0.0	35	0.35	Reversal
0-3			55	0.55	
25-1			18	0.17	Reversal
25-2	25	0.23	35	0.32	No reversal
25-3			50	0.46	Reversal
50-1			35	0.30	
50-2	50	0.43	42	0.36	No reversal
50-3			50	0.43	

Note: $p_c^{'}$ is initial average effective stress

3. ANALYSIS OF EXPERIMENTAL RESULTS

3.1. Development Process Of Dynamic Pore-water Pressure

Figure 1 shows typical history curves of dynamic pore-water pressure during the undrained triaxial test including no static deviator stresses ($q_s / p_c^{'} = 0$), static deviator stresses and deviator stresses reversal ($q_s / p_c^{'} > 0$, and $q_{cyc} > q_s$), static deviator stresses and no deviator stresses reversal, respectively. The deformation and strength characteristics of saturated sand under cyclic loading intensely depend on the behavior of dynamic pore-water pressure. According to the growth rate of dynamic pore-water pressure, development process of dynamic pore-water pressure is classified into the following four stages, initial stage, steady building up stage, rapid building up stage and stable stage, showed as following Figure 1(a), (b) and (c). Initial stage is the first several periods after cyclic loading. The dynamic pore-water pressure sharply builds up during this stage because plastic volume strain developed to a large amount. The steady building up stage is that dynamic pore-water pressure gradually grown by a certain rise rate. However, dynamic pore-water pressure was closely

related with volume strain of soil, including plastic volume strain and elastic volume strain. Both volume strains make different contribution to dynamic pore-water pressure. The elastic volume strain appears a variation tendency of sine curve with cyclic loading, with the result that dynamic pore-water pressure induced by elastic volume strain has a variation tendency of sine curve, too. The plastic volume strain gradually accumulated with cyclic loading so that the development of dynamic pore-water pressure was a gradual accumulation and a variation tendency of sine curve during this stage. Moreover, the arrangement of sand particles is continual readjustment when the sample is subjected to cyclic loading. The soil is in limiting equilibrium state at the moment of load-unload but the phenomenon of destabilization does not occur. When dynamic pore-water pressure gradually accumulates to some degree, there is a tendency of rapid development at the moment. Compared with steady building up stage, there is a bigger growth rate of dynamic pore-water pressure during rapid building up stage. However, in the later period of this stage, some troughs emerge in peak and valley of dynamic pore-water pressure curves. This phenomenon indicates that the destabilization of soil will occur. For stable stage, the peak value of dynamic pore-water pressure is constant and it is shown that failure occurs when the troughs in peak and valley of dynamic pore-water pressure curves are invariant. Figure 1(c) shows that the rapid building up stage does not appear in the dynamic pore-water pressure curve and there is not a obvious trough in peak and valley of the dynamic pore-water pressure curve. The shear dilatation phenomenon is not obvious. Consequently, the sample does not undergo a sudden increase of axial strain.

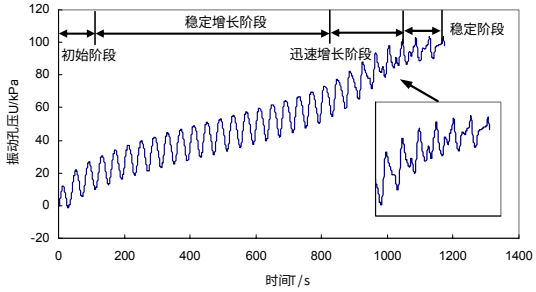

(a) $q_s / p_c^{'} = 0$

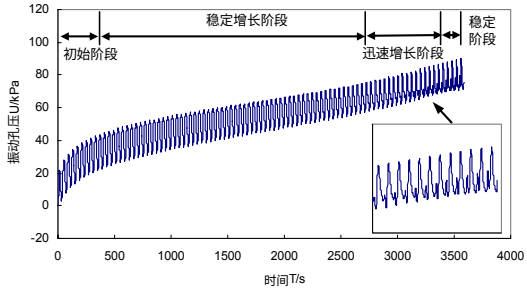

(b) $q_s / p_c^{'} > 0$ and $q_{cyc} > q_s$

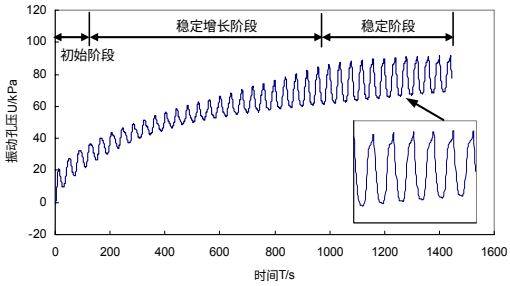

(c) $q_s / p_c^{'} > 0$ and $q_{cyc} < q_s$

Fig.1 Curve of dynamic pore-water pressure

3.2. Effective Stress Path And Failure Pattern

According to the static deviator condition and the deviator stress reversal or non-reversal condition, the effective stress path under cyclic loading was classified into the following three types, (1) $q_s / p_c^{'} = 0$, as shown in Figure 2. (2) $q_s / p_c^{'} > 0$ and $q_{cyc} > q_s$, as shown in Figure 3(b) and Figure 3(c). (3) $q_s / p_c^{'} > 0$ and $q_{cyc} < q_s$, as shown in Figure 3(a) and Figure 4. Figure 2, Figure 3 and Figure 4 show the effective stress path of Nanjing flake-shaped sand subjected to cyclic loading, together with superposition of monotonic test results. The curve of effective stress path from undrained monotonic compression test results is a "S" shape and divided into straightway and elliptical curve by the phase transformation line($\eta_{PT} = q / p^{'} = 1.49$). The stress paths indicate typical character from contractive to dilative and they are divided into three stages by the initial phase transformation line, the phase transformation line and limit phase

line, including the initial compression stage Ⅰ, contractive stage Ⅱ and dilative stage Ⅲ. There is high porosity of sand at the beginning of the test, and pore-water pressure induced by volume contraction of the soil sample increases quickly so that the stress paths moved from the initial point to the origin of coordinates, corresponding to the initial phase of the dynamic pore-water pressure curve as shown in Figure 1(a), (b) and (c). When the stress paths went into the contractive stage Ⅱ, corresponding to the steady building up stage of the dynamic pore-water pressure curve as shown in Figure 1(a), (b) and (c), dynamic pore-water pressure developed gradually under cyclic loading and mean effective stress reduced at a certain rate. At the same time, the stress paths gradually approached to the origin of coordinates. This phenomenon may be found from three kinds of stress paths mentioned above. However, in the later phase of the contractive stage, the mean effective stress decreased rapidly and the effective stress path reached the phase transformation line when the accumulation of pore-water pressure reached a certain degree, and for the effective stress path type 1 and 2, the sample became dilative when deviator stress was reversal. The deviator stress and mean effective stress equal or close to the zero, and this indicates the characteristic of cycle mobility, as shown in Figure 3, Figure 4(b) and Figure 4(c). But for the third type of effective stress path, the soil sample mainly subjected to recycle compression. With accumulation of dynamic pore-water pressure, the effective stress path gradually reached the phase transformation line. After going into the dilative phase region, the stress paths became some overlapped hysteretic loops, as shown in Figure3 and. Figure4.

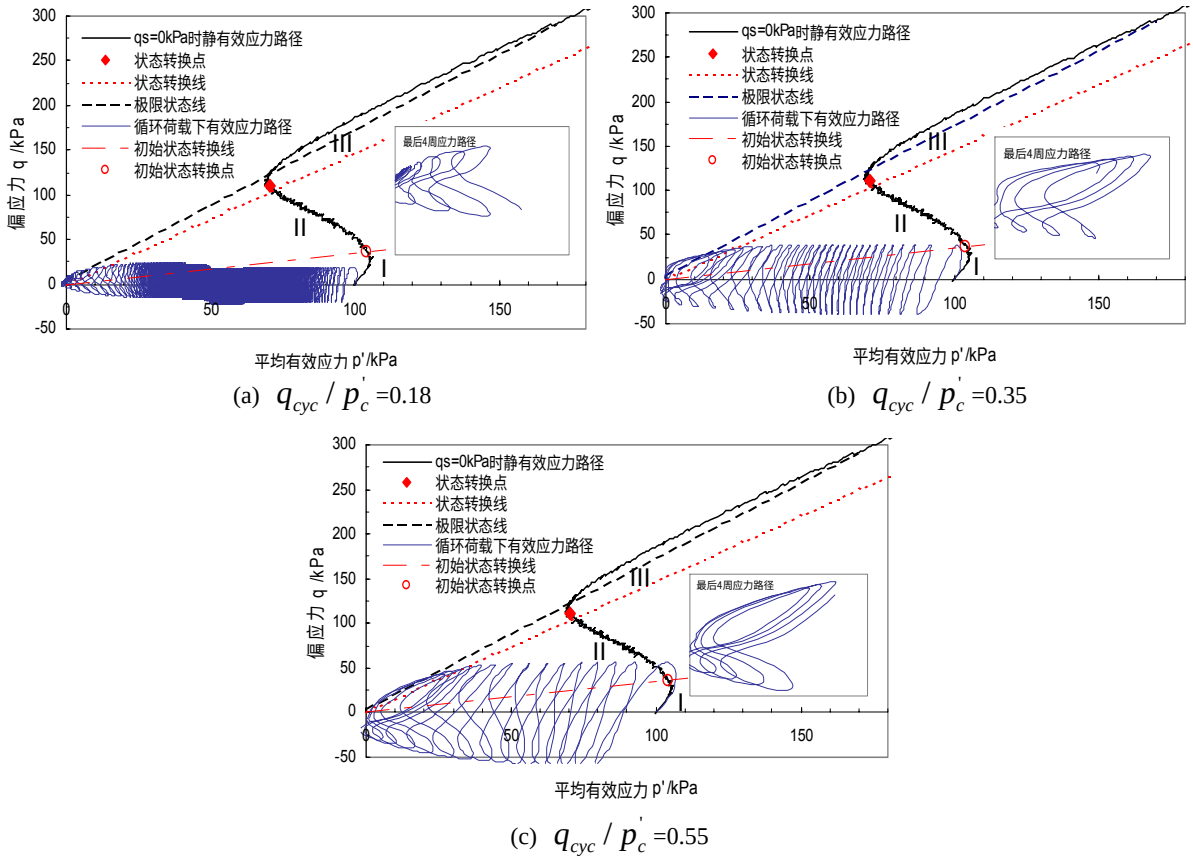

(a) $q_{cyc} / p_c^{'}$ =0.18

(b) $q_{cyc} / p_c^{'}$ =0.35

(c) $q_{cyc} / p_c^{'}$ =0.55

Figure 2 Dynamic behaviors of flake-shaped structural Nanjing fine sand from cyclic triaxial tests without static deviator stress ($q_s / p_c^{'} = 0$)

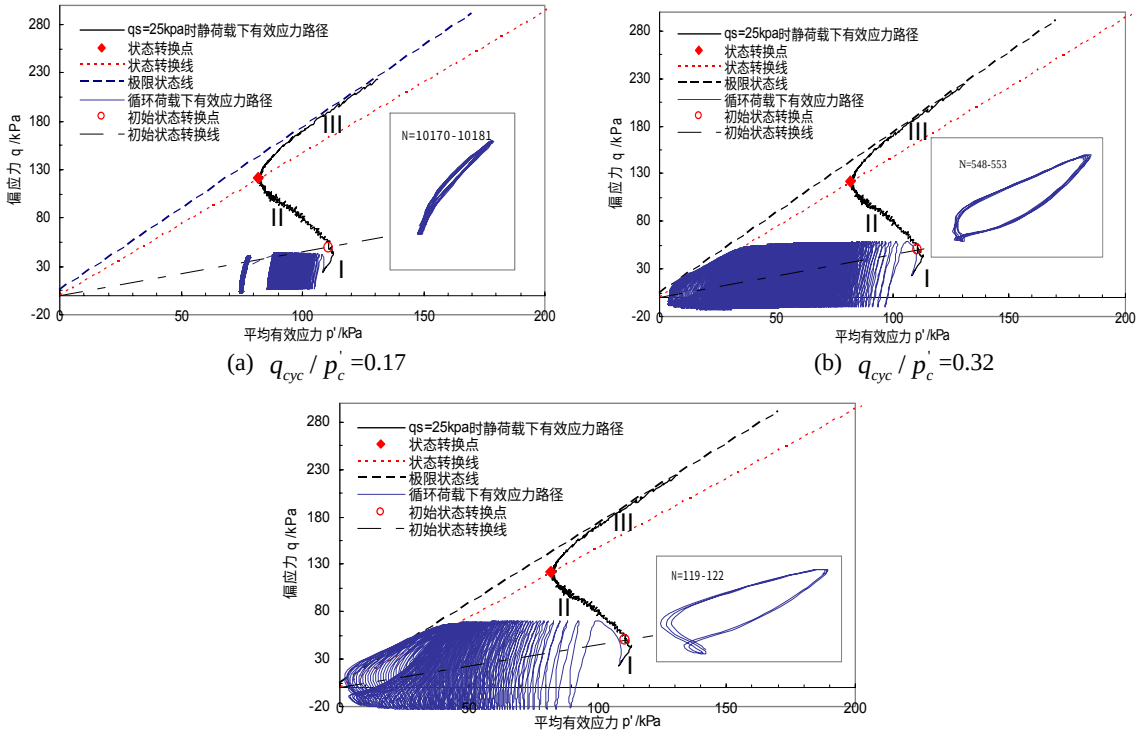

(a) $q_{cyc} / p_c^{'}$ =0.17 (b) $q_{cyc} / p_c^{'}$ =0.32

(c) $q_{cyc} / p_c^{'}$ =0.46

Figure3 Dynamic behaviors of flake-shaped structural Nanjing fine sand from cyclic triaxial tests with static deviator stress ratio $q_s / p_c^{'} = 0.23$

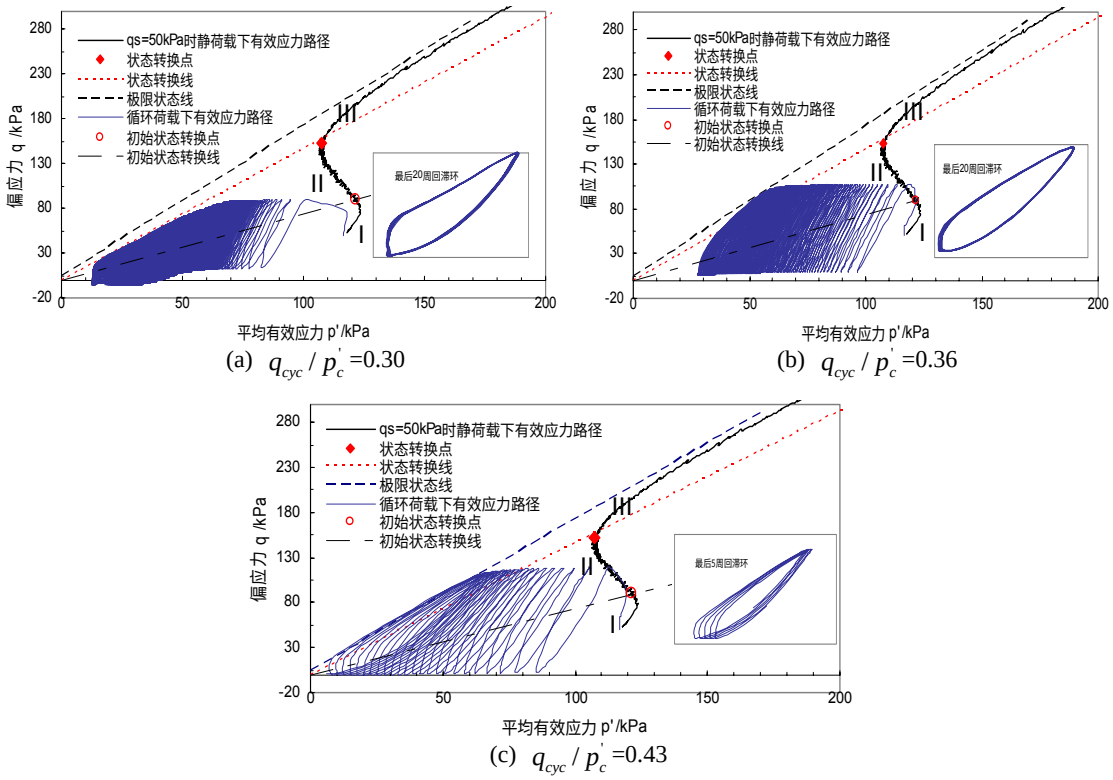

(a) $q_{cyc} / p_c^{'}$ =0.30 (b) $q_{cyc} / p_c^{'}$ =0.36

(c) $q_{cyc} / p_c^{'}$ =0.43

Figure 4 Dynamic behaviors of flake-shaped structural Nanjing fine sand from cyclic triaxial tests with static deviator stress ratio $q_s / p_c^{'} = 0.43$

The cyclic triaxial test results mentioned above show that the failure pattern of Nanjing flake-shaped fine sand

could be divided into two types: (1) cyclic mobility. At the early stage of the test, the sample exhibited very little dynamic strain and with soil sample subjected to continuous cyclic loading，when the effective stress paths gradually approached to origin of coordinates, the axial strain suddenly increased and developed continuously so that the sample tested behaved like a liquid and hence this type of failure can be called liquefaction failure. This type of failure corresponded to the effective stress path type 1 and 2, as shown in Figure 2, Figure 3(b) and Figure 3(c). (2) plastic strain accumulation failure pattern. This type of failure corresponded to the effective stress path type 3. When samples experienced a non-reversal of cyclic stress, accumulation strain played a key role. It can be seen that accumulation failure of plastic strain occurred when the paths reached the phase transformation line(PTL), as shown in Figure 4. However, it is deserved to be mentioned that the accumulation of dynamic pore-water pressure and plastic strain stopped increasing after they were up to a certain value. The effective stress path curve become series of overlapping hysteretic loops and stay away from phase transformation line, as shown in Figure 3 (a).

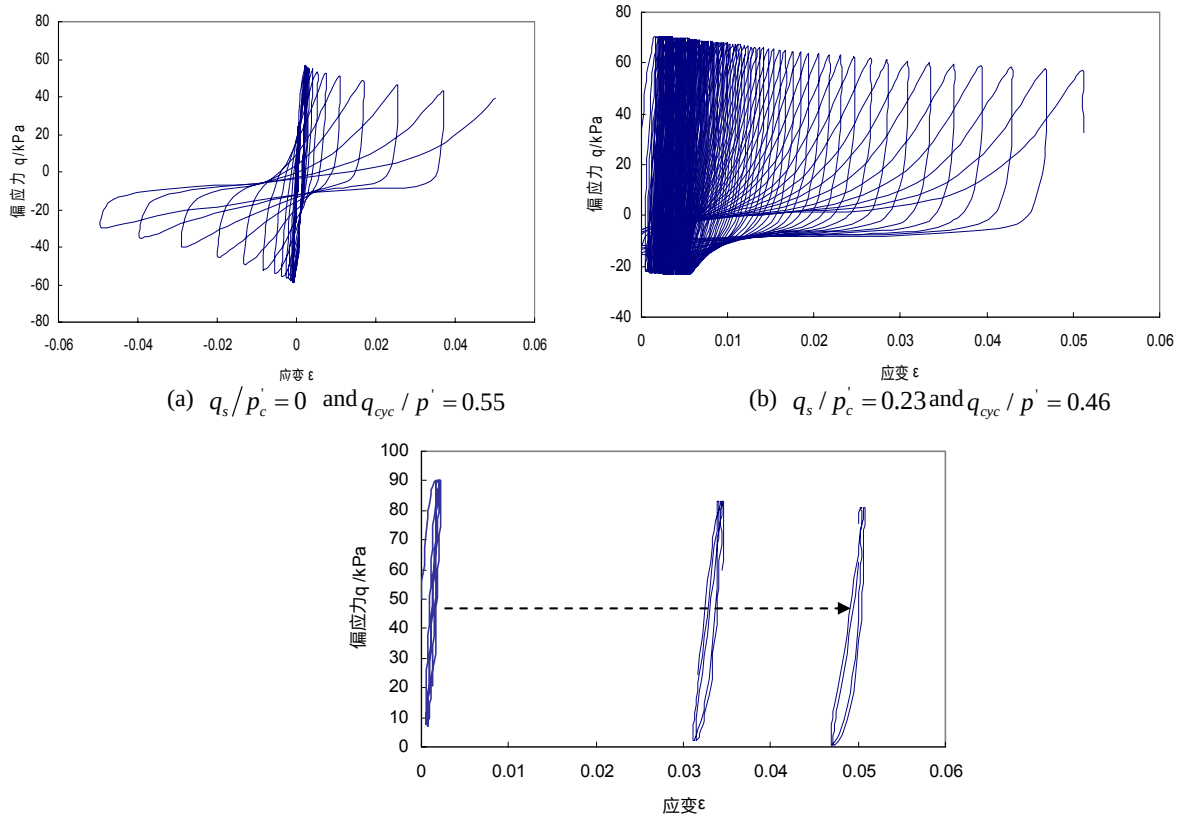

(a) $q_s / p_c^{'} = 0$ and $q_{cyc} / p^{'} = 0.55$

(b) $q_s / p_c^{'} = 0.23$ and $q_{cyc} / p^{'} = 0.46$

(c) $q_s / p_c^{'} = 0.43$ and $q_{cyc} / p^{'} = 0.36$

Figure.5 Typical curves of stress-strain relationship on flake-shaped structural Nanjing fine sand from cyclic triaxial tests with different static deviator stress and dynamic stress

3.3. Stress-Strain Behavior

For the no static deviator stress condition （$q_s / p_c^{'} = 0$） , the cyclic load is symmetrical. When the stress path goes into dilative phase region, the soil sample begins to dilative and its stiffness increase with the effective stress increasing. The curve of the stress-strain relationship is the symmetrical “S” form. The typical stress-strain relationship is indicated in Figure 5(a). However, for the static deviator stress and no deviator stress reversal condition （$q_s / p_c^{'} > 0$ and $q_{cyc} > q_s$） , the cyclic load is unsymmetrical. So, the plastic strain cumulated in one direction and when the stress reverses, the strain increase gradually and the stress-strain hysteretic loops offset gradually. When the stress path comes into dilative phase region after passing phase transformation line, the curve of the stress-strain relationship is symmetrical, and the transient liquefaction

happened at the time when the deviator stress equals to 0. The typical stress-strain relationship is indicated in Figure 5(b). In two situations mentioned above, sand soil began to dilative and pore-water pressure decreased with the increase of deviator stress so that it can get some intensity again. The typical stress path is indicated in Figure 2(c) and 3(c). For the static deviator stress and deviator stress no-reversal conditions （$q_s > p_c^{'}$ and $q_{cyc} > q_s$） , the typical stress-strain relationship is indicated in Figure 5(c). Similarly, the cyclic load is unsymmetrical, and the plastic strain cumulates in one direction and the cumulate strain is dominated and behaved as the stress-strain hysteretic loop shift gently. When the stress path comes into dilative phase region after passing the phase transformation line, the stress-strain hysteretic loop increases but its shape does not change obviously. The typical stress path is indicated in Figure 4(b). The Figure 5(c) also show that the failure pattern of Nanjing flake-shaped sand is plastic strain accumulative failure in the static deviator stress and deviator stress no-reversal condition($q_s / p_c^{'} > 0$ and $q_{cyc} > q_s$).

3.4. Cyclic Mobility

As far as the saturated cohesionless soils concerned, there are three different typical liquefaction mechanisms: sand boil, flow slide and cyclic mobility. From macroscopic view, the cyclic mobility is considered to be concerned with the alternative change between the shear contraction and the shear dilatation in the circulation of the specimen. So it forms the pattern of transient liquefaction and limited intermittent deformation and can be called cyclic mobility. That is saying, dynamic pore-water pressure can achieve the confining pressure, $u = \sigma_3$ or $\sigma_3^{'} = 0$ ($q = 0$ and $p^{'} = 0$) only at some moment during cyclic loading. However, the liquefaction mechanism of cyclic mobility is rather complicated. So a preliminary discussion is done for the cyclic mobility of Nanjing flake-shaped fine sand subjected to cyclic loading.

The effective stress paths are seen in Figure 2, Figure 3 (b) and 3 (c). At the preliminary stage of cyclic loading, dynamic pore-water pressure developed rapidly, caused by the tendency of volume contraction. And the mean effective stress decreased quickly during primary several stress cycle. In the middle and later stage of cyclic loading, the dynamic pore-water pressure decreased with loading and increased with unloading in a cycle. The possible reasons lie in the anisotropy character of the flaky particle structural sand. The well connectivity between the soil particles made dynamic pore-water pressure tend to disappear when the soil specimen is loaded. However, when the soil specimen is unloaded, the connectivity between the soil particles become relaxation and the soil particles have to rearrange for tending to a stable state of Minimum Potential Energy so that the soil is denser. However, during a loading cycle, the pore-water pressure is fluctuation and it can increase and decrease. Only when the cycle is over, the dynamic pore-water pressure can produce a net increasing. When the dynamic pore-water pressure accumulated to some extent, the effective stress path past the phase transformation line to enter the dilative stage. During the progress, the dynamic pore-water pressure decreased when loaded and the increasing phenomenon is more notable when unloaded .After many alternative cycles between shear contraction and shear dilatation, it forms the intermittent transient liquefaction.

4. CONCLUSION

Through the inspection of the cyclic triaxial test on flake-shaped Nanjing fine sand, and the analysis of the test results, the effective stress path in different stages, two failure patterns of flake-shaped Nanjing fine sand, and the stress-stain relationship with different static deviator stress and dynamic stress were analyzed by combining the development of the dynamic pore-water pressure and stress path. And the mechanism of cyclic mobility on flake-shaped Nanjing fine sand was discussed. Conclusions and suggestions are as follows:

(1) The development process of the effective stress path is closely related to cyclic load with or without deviator stress reversal and the occurrence and development of the dynamic pore-water pressure. Meanwhile, static deviator stress has a remarkable effect on the stress path.

(2) According to whether there is deviator stress reversal or not, the failure pattern of flake-shaped Nanjing fine sand could be divided into two types: cyclic mobility and plastic strain accumulation failure pattern. When there is no deviator stress reversal, the destruction of flake-shaped Nanjing fine sand is due to plastic strain accumulation. Meanwhile, when there is deviator stress reversal, its destruction is caused by the rapid

development of cycle strain, performed as the characteristic of cyclic mobility. And the curve of the stress-strain relationship is the symmetrical “S” form. However, if there is no deviator stress reversal, when the cyclic stress is less than a certain level, no matter how much cycles, the sample will not be destructed.

(3) The decrease of dynamic pore-water pressure when loaded and the increase when unloaded, and the alternative cycles between shear contraction and shear dilatation form the cyclic mobility of flake-shaped Nanjing fine sand.

(4) While the railway vibrates, the foundation of flake-shaped Nanjing fine sand is mainly under the state of one-way compressive with no deviator stress reversal, which belongs to plastic strain accumulation failure pattern. It should fully draw the attention of the traffic roadbed design offices and the construction cector.

REFERENCES

Zhou Jing. (1999), The engineering properties of Nanjing sand—Report on reinforce techniques for Nanjing bridge of Yangtze River. China Railway publishing House.

CHEN Wen-hua, SUN Mou, LIU Ming-li, et al. (2003), Characters of schistose structure of Nanjing's sand and seismic liquefaction of subsoil of a metro section. *Rock and Soil Mechanics*,**24:5**, 755-758

Chen Guo-xing, Liu Xue-zhu. (2004), Testing study on ratio of dynamic shear moduli and ratio of damping for deposited soils in Nanjing and its neighboring areas. *Chinese Journal of Rock Mechanics and Engineering*, **23:8**, 1403-1410

CHENG Jian-jun, YAN San-bao, JIANG Jian-ping, et al. (2004), Assessment on the main engineering geological problems in the south-north line of Nanjing metro. *Journal of Earth Science and Enivronmental*, **26:1**, 46-51

Liu ying, Xie jun-fei. (1984), Dynamic liquefaction of sand soil. Beijing: Seismological Press

Wang Wen-shao. (2005), Distinction and interrelation between liquefaction, state of limit equilibrium and failure of soil mass. *Chinese Journal of Geotechnical Engineering*, **27:1**,1-10